Constraints on the CMB temperature-redshift dependence from SZ and distance measurements

JCAP02(2012)013

(http://iopscience.iop.org/1475-7516/2012/02/013)

Journal of Cosmology and Astroparticle Physics
An IOP and SISSA journal

Constraints on the CMB temperature-redshift dependence from SZ and distance measurements

A. Avgoustidis,[a,b] **G. Luzzi,**[c] **C.J.A.P. Martins**[d] **and A.M.R.V.L. Monteiro**[d,e]

[a]School of Physics and Astronomy, University of Nottingham, University Park, Nottingham NG7 2RD, England
[b]Centre for Theoretical Cosmology, DAMTP, CMS, Wilberforce Road, Cambridge CB3 0WA, England
[c]Laboratoire de l'Accélérateur Linéaire, Université de Paris-Sud, CNRS/IN2P3, Bâtiment 200, BP 34, 91898 Orsay Cedex, France
[d]Centro de Astrofísica, Universidade do Porto, Rua das Estrelas, 4150-762 Porto, Portugal
[e]Faculdade de Ciências, Universidade do Porto, Rua do Campo Alegre 687, 4169-007 Porto, Portugal
E-mail: A.Avgoustidis@damtp.cam.ac.uk, gluzzi@lal.in2p3.fr, Carlos.Martins@astro.up.pt, up090322024@alunos.fc.up.pt

Received December 10, 2011
Accepted January 16, 2012
Published February 14, 2012

Abstract. The relation between redshift and the CMB temperature, $T_{\rm CMB}(z) = T_0(1+z)$ is a key prediction of standard cosmology, but is violated in many non-standard models. Constraining possible deviations to this law is an effective way to test the ΛCDM paradigm and search for hints of new physics. We present state-of-the-art constraints, using both direct and indirect measurements. In particular, we point out that in models where photons can be created or destroyed, not only does the temperature-redshift relation change, but so does the distance duality relation, and these departures from the standard behaviour are related, providing us with an opportunity to improve constraints. We show that current datasets limit possible deviations of the form $T_{\rm CMB}(z) = T_0(1+z)^{1-\beta}$ to be $\beta = 0.004 \pm 0.016$ up to a redshift $z \sim 3$. We also discuss how, with the next generation of space and ground-based experiments, these constraints can be improved by more than one order of magnitude.

Keywords: cosmology of theories beyond the SM, high redshift galaxies, Sunyaev-Zeldovich effect, baryon acoustic oscillations

ArXiv ePrint: 1112.1862

doi:10.1088/1475-7516/2012/02/013

JCAP02(2012)013

Contents

JCAP02(2012)013

1 Introduction

Cosmology and particle physics are presently experiencing a truly exciting period. On the one hand, both have remarkably successful standard models, which are in agreement with a plethora of experimental and observational data. On the other hand, there are also strong hints that neither of these models is complete, and that new physics may be there, within the reach of the next generation of probes.

There are three compelling and firmly established observational facts that the standard model of particle physics fails to account for: neutrino masses, the existence of dark matter, and the size of the baryon asymmetry of the Universe. For each of these, the model makes very specific statements, failing however to reproduce the experimental evidence. It is precisely our confidence in the model and our ability to calculate its consequences that lead us to the conclusion that it is incomplete, and new phenomena must be anticipated. This is, of course, the reason for the LHC project.

Similarly, the last decade saw the emergence of the so-called concordance model of cosmology. This can reproduce all the available observations with only a small number of parameters, but also requires that about 96% of the content of the universe is in a form that has never been seen in the laboratory (and is only known indirectly from its gravitational properties). It is thought that dark matter is a subdominant part of this, while the dominant one is an even more mysterious component usually called dark energy.

In this context, it is important to identify laboratory or astrophysical probes that can give us more information about the nature and properties of this still unknown physics. In this work we will discuss one such probe — the temperature-redshift relation —, and lay the foundations for exploring its cosmological implications.

One of the most precise measurements in cosmology is the intensity spectrum of the cosmic microwave background radiation: the COBE-FIRAS experiment revealed a very precise black-body spectrum [1]. However, this measurement tells us nothing about the behaviour of the Cosmic Microwave Background (CMB) at non-zero redshift. If the expansion of the Universe is adiabatic and the CMB spectrum was a black-body at the time it originated, this shape will be preserved with its temperature evolving as $T(z) = T_0(1 + z)$. This is a robust prediction of standard cosmology, but it is violated in many non-standard models, including string theory motivated scenarios where photons mix with other particles such as axions (see [2] for a recent review), and those where dimensionless couplings like the fine-structure constant vary [3].

A few measurements of $T(z)$ already exist, but the currently large uncertainties do not allow for strong constraints on the underlying models to be set. However, with future datasets this will become a competitive probe. It is therefore timely to discuss what these measurements can tell us about the underlying cosmological paradigms.

At low redshifts, say $z < 1$, the $T(z)$ relation can be measured via the Sunyaev-Zeldovich (SZ) effect towards galaxy clusters. This method was applied to ground-based CMB observations [4, 5], which demonstrated its potential. With a new generation of ground experiments becoming operational and a forthcoming all-sky survey of SZ clusters to be carried out by Planck [6], the potential of this method will come to fruition. At higher redshifts, $z > 1$, $T(z)$ can be evaluated from the analysis of quasar absorption line spectra which show atomic and/or ionic fine structure levels excited by the photon absorption of the CMB radiation [7]. (The CMB is an important source of excitation for species with transitions in the submillimeter range.) Although the suggestion is more than four decades old, measurements (as opposed to upper bounds) were only obtained in the last decade, and the best ones so far still have errors at the ten percent level [8].

Here we will study these issues in detail, but we will also place them in a wider context. For example, in models where photons can be created or destroyed, not only does the temperature-redshift relation vary, but so does the distance duality relation (also known as the Etherington relation [9]), and these two different departures from the standard behaviour are quantitatively related. One issue that has been overlooked so far is that in such models, where photon number is not conserved, this relation between $T(z)$ and distance duality provides us with an opportunity to improve constraints. By combining data from different observations one not only reduces the statistical uncertainties on underlying phenomenological parameters but, given the different nature of both observational datasets, one also has a much better control over possible systematics.

We therefore discuss in detail the origin of the above relation, as it can be a unique consistency test for the standard paradigm and, at the same time, a valuable tool for probing new physics beyond the standard model. We also study further imprints of these models in the CMB, and present forecasts for improvements that Planck, as well as planned Baryon Acoustic Oscillations (BAO) missions and spectrographs planned for the VLT and the E-ELT, will soon make possible. Last but not least, we derive the strongest constraints to date on deviations of these relations from their standard behaviour, and quantify the improvements to be expected from the aforementioned forthcoming experiments.

JCAP02(2012)013

2 Theoretical motivation

There are several examples of non-standard, but theoretically well-motivated, physical processes that could affect the cosmological temperature-redshift relation. Constraining deviations from the standard law $T(z) = T_0(1+z)$ therefore provides a invaluable tool for probing physical theories. Examples of scenarios that could be constrained include decaying vacuum cosmologies/photon injection mechanisms, couplings between photons and axion-like particles, modified gravity scenarios, and so on. In this section, we discuss two examples of how these models affect the $T(z)$ relation.

2.1 Adiabatic photon injection

Naively, the most obvious way to violate the $T(z) = T_0(1+z)$ relation is when there is energy injection into the CMB (say from a decaying scalar field) or, conversely, when photons are destroyed. The Planckian form of the spectrum is preserved if photon creation is adiabatic, that is, if the entropy per photon remains constant. Lima et al. [10, 11] have studied this in the context of decaying vacuum cosmologies; here we review some of their formalism.

Generically, such a process of particle creation can be described by saying that the energy density evolves as

$$\dot{\rho} + 3H(\rho + p) = C \tag{2.1}$$

while the particle number density obeys

$$\dot{n} + 3Hn = \Psi\,, \tag{2.2}$$

where C, Ψ are real functions of time. Deviations from particle number conservation can then be quantified by the phenomenological parameter

$$0 \leq \beta \equiv \frac{\Psi}{3Hn} \leq 1\,, \tag{2.3}$$

which can be time-dependent.

In general the temperature evolves as [10, 11]

$$\frac{\dot{T}}{T} = \left(\frac{\partial p}{\partial \rho}\right)_n \frac{\dot{n}}{n} - \frac{\Psi}{nT(\partial\rho/\partial T)_n}\left[\rho + p - \frac{nC}{\Psi}\right], \tag{2.4}$$

but note that the second term is zero if C and Ψ are related by

$$C = \frac{\rho + p}{n}\Psi\,, \tag{2.5}$$

or, in terms of the parameter defined in (2.3), $C = 3H(\rho + p)\beta$. This corresponds to adiabaticity: the specific entropy per particle of the created particles remains constant, so new particles are actually created in equilibrium with already existing ones. In this case the temperature evolution equation reduces to

$$\frac{\dot{T}}{T} = \left(\frac{\partial p}{\partial \rho}\right)_n \frac{\dot{n}}{n}\,, \tag{2.6}$$

as in the standard cosmological model. Recall that, in the standard model, both the equilibrium relations and the Planckian form of the spectrum for photons are preserved in the

JCAP02(2012)013

course of expansion. The former can be seen directly from equation (2.6), while the latter is the result of the kinematical condition for FRW geometry, $\nu \propto a^{-1}$, and of photon number conservation, which together imply $T \propto a^{-1}$ (away from mass thresholds). With adiabatic photon creation, equation (2.6) remains valid — as we just saw — and thus the equilibrium relations are preserved.

Indeed, if one considers the generic equation of state $p = (\gamma - 1)\rho$ one can integrate the above equations to get

$$T \propto n^{\gamma-1}, \qquad \rho \propto n^{\gamma}. \tag{2.7}$$

However, since the entropy per photon is conserved, the temperature now obeys

$$\frac{Ta}{N^{1/3}} = \text{const}\,, \tag{2.8}$$

where $N(z)$ is the comoving photon number, which changes in time as new photons are being injected in equilibrium. It then follows that the dimensionless frequency relevant for the SZ effect (to be considered in section 4) evolves as

$$x = x_0(1+z)\frac{T_0}{T_{\rm CMB}}\,, \tag{2.9}$$

with

$$T_{\rm CMB} = T_0(1+z)\left[\frac{N(z)}{N_0}\right]^{1/3}. \tag{2.10}$$

Thus, it is now $h\nu(N/N_0)^{1/3}/kT$ in the exponential of the photon distribution function that stays constant during cosmological evolution, and so a generalised Planck-type spectrum [10] is preserved, which is why the equilibrium relations are still recovered, e.g. $\rho \propto T^4$ for a radiation fluid (where the proportionality factor is the radiation density constant).

Although one cannot distinguish at present the usual Planckian spectrum from such a generalised one, this is not necessarily true at higher redshifts. For example, the wavelength λ_m of the peak of the distribution is now

$$\lambda_m\, T = 0.289\left[\frac{N(z)}{N_0}\right]^{1/3}, \tag{2.11}$$

which is a generalisation of Wien's law (and naturally reduces to it in the standard case). This could in principle be observationally tested.

We can illustrate these points with two simple examples. Assuming a radiation fluid, $p = \rho/3$ we have

$$\frac{\dot{T}}{T} = -H + \frac{\Psi}{3n} = -H + \frac{C}{4\rho} \tag{2.12}$$

and for a constant β we find

$$\dot{\rho} + 4(1-\beta)H\rho = 0 \tag{2.13}$$

$$\dot{n} + 3(1-\beta)Hn = 0 \tag{2.14}$$

$$T(z) = T_0(1+z)^{1-\beta}\,; \tag{2.15}$$

the dimensionless frequency is therefore

$$\frac{x}{x_0} = (1+z)^{\beta}. \tag{2.16}$$

JCAP02(2012)013

For a more general equation of state $p = (\gamma - 1)\rho$ we have

$$T \propto a^{-3(\gamma-1)(1-\beta)}. \tag{2.17}$$

Thus, for any given redshift the temperature of the expanding universe is slightly lower than in the standard case. This is the phenomenological parameterisation that has been used by almost all previous authors. Note that for many realistic models this is not an accurate description (as β is in general time-dependent), but it is adequate at sufficiently low redshifts. Since, currently, cluster data probe down to redshifts less than unity with sensitivities in temperature of order a few percent or worse (see section 4), we will adopt this parameterisation for the purposes of the present paper (but will revisit the issue in a follow-up publication). As cosmological data improve and extend to higher redshifts (see section 6), time variation of the parameter β will also be constrained.

2.2 Photon dimming/absorption & axion-photon couplings

The effect of photon dimming/absorption can arise in a wide range of astrophysical and high-energy physics scenarios, ranging from photon absorption by grey dust to photon conversion into a different particle species, like for example photon-to-axion conversion in the presence of a magnetic field.

Grey dust has been invoked as an alternative explanation of the observed dimming of Type Ia Supernovae [12], but it is now understood that it cannot fit high redshift data (like for example the Union sample [13]) by itself, i.e. without some contribution from a cosmological constant-like fluid [14]. Axion-Like-Particles (ALPs), on the other hand, arise in a wide range of well-motivated high-energy physics scenarios, including string theoretic models where ALPs appear as zero modes of various antisymmetric form fields [15]. Like dust, they can lead to dimming of Type Ia Supernovae [16], but this cosmological scenario is also strongly constrained [17, 18, 22]. For a recent review of ALPs and related laboratory, astrophysical and cosmological constraints, see [2].

Irrespectively of its microphysical origin, photon dimming violates photon number conservation, and so it can be described macroscopically in a very similar way to photon injection, by simply allowing the parameter β in equation (2.3) to be negative. In particular, the balance (2.14) and temperature evolution (2.6) equations are valid with constant negative β (note that, as before, constant β is only an approximation) and the temperature-redshift relation is again:

$$T(z) = T_0(1+z)^{1-\beta}. \tag{2.18}$$

Crucially for this work, violations of photon number conservation also give rise to deviations from the standard relation [9] between luminosity and angular diameter distance, which can be independently constrained [14, 22–25]. With current data, it is sufficient to parameterise the luminosity-angular diameter distance relation as:

$$d_L(z) = d_A(z)(1+z)^{2+\epsilon}, \tag{2.19}$$

where ϵ is constant. The value $\epsilon = 0$ corresponds to the standard $d_L - d_A$ law. Since ϵ and β are related by the underlying physical model but can be constrained independently through measurements of very different systematics, this provides a very promising tool for carrying out a consistency test of the standard cosmological scenario and constraining physics beyond the standard model. However, such complementary measurements often cover a very different wavelength range so one must be careful when comparing direct and indirect

JCAP02(2012)013

constraints. For example, if one uses Supernova (SN) data to constrain the parameter ϵ at optical wavelengths within a model of chromatic axion-photon mixing, one should take into account the wavelength dependence of the model when translating this bound into a constraint in the CMB temperature-redshift relation. In general, one may expect photon-dimming to be stronger at high photon energies, so indirect bounds on $T(z)$ coming from SN brightness measurements can be assumed to be conservative. In section 5 we will present the constraints obtained from such an analysis with current data, and in section 6 we examine the prospects of improving these constraints by future SN and BAO data.

In passing, we note that another way to see that the temperature-redshift relation becomes modified in models violating photon number conservation is by considering the more obvious effect of the distance-duality violation in these models. The source of this distance-duality violation is the difference between the true and observed (dimmed) photon flux, which tricks one to infer a larger luminosity distance. As flux scales inversely with the luminosity distance squared, this change in the inferred distance would also affect the CMB flux-redshift relation, and so the CMB temperature as a function of redshift.

Before moving to the study of the various constraints imposed on β and ϵ, let us explore their relation in more detail. Consider the CMB spectrum in the presence of a dimming agent, like for example photon absorption due to a dust field or conversion into ALPs. Imagine that the spectrum is Planckian at the epoch T so that the the number of photons per unit volume per frequency interval is:

$$n(\nu)d\nu = \frac{8\pi}{c^3}\frac{\nu^2 d\nu}{e^{h\nu/kT}-1}\,. \tag{2.20}$$

If photon number was conserved, then at a later epoch T' the number density per frequency interval, $n'(\nu')d\nu'$, would be related to (2.20) through the volume rescaling $(a/a')^3$; this can be absorbed as frequency dependence, $\nu' = (a/a')\nu$, yielding the standard result of a Planckian spectrum $n(\nu')d\nu'$ of temperature $T' = (a/a')T$. With dimming, however, photons can be lost in flight and the spectrum will generally be distorted. Introducing a photon survival fraction $f_{\rm surv} \lesssim 1$ between the epochs T and T' we now have:

$$n'(\nu')d\nu' = f_{\rm surv}\, n(\nu)d\nu(a/a')^3 = \frac{8\pi}{c^3}\frac{f_{\rm surv}\,\nu'^2 d\nu'}{e^{h\nu'/kT'}-1} \lesssim n(\nu')d\nu',$$

where, as before, $\nu' = \nu(a/a')$ and $T' = (a/a')T$. Thus the spectrum is distorted. However, if the photon survival fraction does not depend on frequency (of course, it can — and generally will — depend on redshift), then one can change variables to $\nu'' = (f_{\rm surv})^{1/3}\,\nu'$, yielding:

$$n'(\nu')d\nu' = n(\nu'')d\nu'',$$

that is, a Planckian spectrum of temperature $T'' = (f_{\rm surv})^{1/3}\,T' = (a/a')(f_{\rm surv})^{1/3}\,T$. This is the 'generalised' Planck distribution of reference [10], discussed in the previous section. In fact, remembering that T' corresponds to an epoch later than T, we have:

$$T(z) = (f_{\rm surv})^{-1/3}(1+z)T_0\,. \tag{2.21}$$

The relation between dimming and temperature distortion then becomes clear. In the parameterisation (2.15), we have $(f_{\rm surv})^{1/3} = (1+z)^\beta$, with β negative. On the other hand, the photon survival probability $f_{\rm surv}$ enters linearly the luminosity, so the luminosity distance scales as $(f_{\rm surv})^{-1/2}$. Therefore, from equation (2.19) it follows that the photon survival

JCAP02(2012)013

probability corresponds, in the ϵ-parameterisation, to $f_{\rm surv} = (1+z)^{-2\epsilon}$. Thus, the relation between the parameter β of equation (2.15) and ϵ of references [14, 22] is simply:

$$\beta = -\frac{2}{3}\epsilon\,. \tag{2.22}$$

Note that in the above discussion we have assumed that the photon survival probability is independent of wavelength, which guaranteed a simple thermal spectrum. Deviations of the CMB from a thermal spectrum have been constrained down to the 10^{-4} level by the COBE-FIRAS measurements, both in the case of a Comptonised spectrum and of a Bose-Einstein spectrum with non-trivial chemical potential [1, 26]. This dataset has also been used recently to constrain frequency-dependent dimming in the context of photon-axion couplings [18] (see also [19–21]). Finally, we have assumed a simple redshift dependence, parameterised by equation (2.19) with constant ϵ. Again, like in the case of constant β (section 2.1), this is justified given current error bars in distance determination and the limited redshift range currently covered, $0 \lesssim z \lesssim 2$ [14]. Forecasts for future data will be discussed in section 6.

3 Constraints from quasar absorption line spectra

The most accurate value of the local CMB temperature measured by the COBE experiment is [1]

$$T_{\rm CMB} = 2.725 \pm 0.002\,{\rm K}\,, \qquad z = 0\,. \tag{3.1}$$

Additional local but extrasolar values of the background radiation temperature can be estimated from observations of interstellar molecular clouds [27] and of the Magellanic Clouds [28]. These extrasolar and extragalactic values are in good agreement with the COBE estimation. Cosmological models predicting non-Planckian spectra of the background radiation at $z = 0$ can be ruled out if they deviate by more than about 1% from the blackbody spectrum. However, these local observations do not allow one to distinguish between the standard model and cosmological models with a blackbody spectrum but different $T(z)$ dependences.

At low redshifts ($0 < z < 1$), the functional scaling of the CMB temperature can be estimated from measurements of the Sunyaev-Zeldovich effect in the direction to clusters of galaxies, as will be discussed in the next section. At higher redshifts ($z > 1$), the CMB temperature can be evaluated from the analysis of quasar absorption line spectra which show atomic and/or ionic fine structure levels excited by the photo-absorption of the CMB radiation. This is an important source of excitation for those species with transitions in the sub-millimetre range. This is the case for atomic species whose ground state splits into several fine-structure levels (and also for molecules that can be excited in their rotational levels, see below). If the relative level populations are thermalised by the CMB, then the excitation temperature gives the temperature of the black-body radiation.

It has long been proposed to measure the relative populations of such atomic levels in quasar absorption lines to derive $T_{\rm CMB}$ at high redshift [29]. The most suitable are the fine structure levels of the ground states of CI $(3P0, 1, 2)$ and CII $(2P1/2, 3, 2)$ showing an energy separation between 24 K and 91 K. The CI lines were used to obtain several upper limits, until advances in instrumentation and analysis techniques allowed actual measurements, starting with Srianand et al. [7] who obtained

$$T_e = 10 \pm 4\,{\rm K}\,, \qquad z = 2.338\,. \tag{3.2}$$

JCAP02(2012)013

To distinguish the contribution to the relative population of the fine-structure levels of the ground state of CI from competing excitation processes the independent analysis of the molecular hydrogen UV absorption lines is important; H_2 transitions from different low rotational levels may be used to infer the UV radiation field and the gas density in the CI-H_2 absorbers. These techniques have so far allowed measurements to be made beyond $z = 3$; the earliest currently available measurement is that of Molaro et al. [30]

$$T_e = 12.1^{+1.7}_{-3.2}\,\mathrm{K}\,, \qquad z = 3.025\,. \tag{3.3}$$

Molecular rotational transitions may also be used to constrain the cosmological temperature-redshift law. So far, absorption and emission lines of CO, OH, CS, HCN, HCO^+, H_2O, NH_3, and other molecules have been observed in distant galaxies and quasars up to $z = 6.42$ (see [31] for a review). The absorption line observations are most suitable to the radiation temperature estimates since, as a rule, molecular absorption arises in the gas components with the lowest kinetic temperatures. Srianand et al. [32] reported the first detection of CO in a high-redshift damped Lyman-α system, while also detecting H_2 and HD molecules. The CO rotational excitation temperatures are higher than those measured in our Galactic ISM for similar kinetic temperature and density. Using the CI fine-structure absorption lines, they show that this is a consequence of the excitation being dominated by radiative pumping by the cosmic microwave background radiation, and from the CO excitation temperatures they derive

$$T_e = 9.15 \pm 0.72\,\mathrm{K}\,, \qquad z = 2.418\,. \tag{3.4}$$

Finally, Noterdaeme et al. [8] have recently reported on a sample of five CO absorption systems where the CMB temperature has been measured. We refer the reader to this work for further details as well as for some more of the history of these measurements and an up-to-date list of all the available ones. They also used their sample, in combination with measurements from the SZ effect, to place constraints on the phenomenological parameter β — we will describe this in the next section.

4 Constraints from the SZ effect towards clusters

The possibility of determining $T_{\rm CMB}(z)$ from measurements of the Sunyaev-Zeldovich effect has been suggested long ago [33, 34]. The effect — Compton scattering of the CMB by hot intracluster (IC) gas — is a small change of the CMB spectral intensity, ΔI, which depends on the integrated IC gas pressure along the line of sight to the cluster. The steep frequency dependence of the change in the CMB spectral intensity, ΔI, due to the SZ effect allows the CMB temperature to be estimated at the redshift of the cluster.

The differential SZ signal may be written at the redshift of the cluster, including relativistic corrections as:

$$\Delta I(z) = \frac{2\big(kT_{\rm CMB}(z)\big)^3}{(hc)^2}\frac{x^4 e^x}{(e^x-1)^2}\tau\big[\theta f_1(x) - v_z/c + R(x,\theta,v_z/c)\big]\,, \tag{4.1}$$

where $\Delta I(z)$ is the brightness change between the centre of the cluster and blank sky, as measured at redshift z, τ is the optical depth, $T_{\rm CMB}(z)$ is the CMB temperature at redshift z, $x = \frac{h\nu(z)}{k_B T_{\rm CMB}(z)}$, $\theta = k_B T_e/m_e c^2$ with T_e electron cluster temperature, v_z the radial component of the peculiar velocity of the cluster, and the $R(x,\theta,v_z/c)$ function includes relativistic corrections.

If we assume that $T_{\rm CMB}$ scales with z as $T_{\rm CMB}(z) = T_{\rm CMB}(0)(1+z)^{1-\beta}$, while the frequency scales as $(1+z)$ as usual, then $\Delta I(z)$ scales like $(1+z)^{3(1-\beta)}$ and we obtain, at the level of the solar system

$$\Delta I(0) = \frac{2\big(kT_{\rm CMB}(0)\big)^3}{(hc)^2}\frac{x'^4 e^{x'}}{(e^{x'}-1)^2}\tau\big[\theta f_1(x') - v_z/c + R(x',\theta,v_z/c)\big]\,, \tag{4.2}$$

where $x' = \frac{h\nu(0)}{k_B T^*_{\rm CMB}}$ and $T^*_{\rm CMB} = T_{\rm CMB}(0)(1+z)^{-\beta}$ will be slightly different from the local temperature $T_{\rm CMB}(0)$ as measured by COBE. In this way it is possible to measure the temperature of the CMB at the redshift of the cluster, thus directly constraining scenarios like those discussed in the previous section.

Let us consider the bound on β coming from $T_{\rm CMB}(z)$ constraints, at redshifts in the range $z = 0.023$–0.546, from multi-frequency measurements of the SZ effect towards the 13 clusters of ref. [5]. By fitting the $T_{\rm CMB}(z)$ data points and relaxing the condition of a positive prior on β, that is allowing for photon dimming/absorption (corresponding to $\beta < 0$) as well as photon creation ($\beta > 0$), we get $\beta = 0.065 \pm 0.080$.

By adding these measurements to higher-redshift ones coming from spectroscopic measurements (discussed in the previous section) involving atomic carbon and CO absorption lines along the line of sight of quasars, ref. [8] subsequently improved the constraints on β, obtaining[1]

$$\beta = -0.007 \pm 0.027\,. \tag{4.3}$$

Despite the higher precision of $T_{\rm CMB}(z)$ measurements from the SZ method with respect to that of the quasar absorption lines method, the present improvement on the constraints on the parameter β depends mainly on the higher lever arm due to the exploration of the distant universe, thanks to the observation of high redshift absorbers. As we will show in section 6.1 forthcoming datasets will soon lead to tighter constraints.

5 Constraints from distance measurements

As briefly alluded to in section 2, an indirect way for constraining the temperature-redshift dependence is through the study of possible deviations from the duality relation [9] between luminosity and angular diameter distance:

$$d_L(z) = (1+z)^2 d_A(z)\,. \tag{5.1}$$

This equation holds for general metric theories of gravity, where photons travel along unique null geodesics, as long as photon number conservation and local Lorentz invariance are respected. Since Lorentz violations are strongly constrained at low energies [35], and in particular at optical wavelengths, the determination of d_L from SN observations can be used [14, 22–25] together with other distance measurements in order to place direct bounds on photon number violation through eq. (5.1). Physically, such a violation can arise from photon absorption, e.g. grey dust [12], or from more exotic effects like photon conversion into axions [16].

[1] Repeating their fit to parameter β we find an uncertainty of 0.028 rather than 0.027; this is likely due to round-off errors in the temperature measurements used as input. The difference is insignificant for the purposes of our subsequent analysis, but for the sake of consistency with the pipeline for comparing to future measurements we will use 0.028 in figures 10 and 11.

JCAP02(2012)013

Systematic violations of (5.1) give rise to an apparent opacity effect in the observed luminosity distance. Indeed, if photons were lost along the line of sight, the inferred luminosity distance would be related to the true one through a multiplicative factor:

$$d^2_{L,\mathrm{inf}} = d^2_{L,\mathrm{true}} e^{\tau(z)}. \tag{5.2}$$

Note that the 'opacity' $\tau(z)$ can be negative, allowing for apparent brightening of the source, as would be the case, for example, if exotic particles were also emitted from the source and later converted into photons [36].

As discussed in section 2, photon number violation would also give rise to a corresponding distortion of the photon temperature-redshift relation, and this allows us to combine different observational probes to constrain such models.

In references [14, 22] the authors used Type Ia SN data (specifically the Union 2008 dataset [13]) in combination with measurements of cosmic expansion $H(z)$ from differential ageing of luminous red galaxies [37–39], and obtained constraints on opacity up to $z \simeq 2$ through equations (5.1)–(5.2). In the simplest case, one can adopt the parameterisation:

$$d_L(z) = d_A(z)(1+z)^{2+\epsilon}, \tag{5.3}$$

allowing violations of eq. (5.1) through a single parameter, ϵ. For low redshifts, this parameter can be directly translated into an opacity function $\tau(z)$ as it simply corresponds to the first term in the Taylor expansion $\tau(z) = 2\epsilon z + \mathcal{O}(\epsilon z^2)$. Different parameterisations were also considered in [22], corresponding to specific theoretical models of opacity such as photons mixing with massless axion-like particles, chameleons and mini-charged particles.

If an opacity source like photon-axion mixing affects SN observations, it should also have an impact on CMB photons. From the above discussion (and that of section 2.2) it is then clear that constraints like those in [14, 22] can be used to place indirect bounds on possible deviations from the standard temperature-redshift law, as expressed, for example, in eq. (2.15). In particular, if opacity is achromatic, which can be the case, for example, for photon-axion mixing in sufficiently low intergalactic electron densities [43], the parameterisation (5.3) corresponds simply to $\beta = -2\epsilon/3$, as we saw in section 2.2. More generally, however, the effective opacity can be expected to be smaller at low energies, so that distance duality violation bounds yield conservative constraints for the allowed CMB temperature-redshift distortion. There are also other bounds on photon-axion mixing, coming from constraining spectral distortions of the CMB radiation [18]. Note that for CMB photons to be converted into axions, a background magnetic field is required at the corresponding redshift. Therefore, the bound on the parameter ϵ constrains a combination of the background magnetic field and the axion-photon coupling [17, 18, 22] (and at the same time, through its relation (2.22) to β it places an indirect constraint on the variation of $T(z)$ as discussed above). Intergalactic magnetic fields have not been directly observed but there are hints that they exist [40]. For further discussion and relevant constraints, see [41, 42]. Finally, note that axions can also convert back into photons — a second order effect which could be significant for large mixing probability.

Let us consider the constraint on β coming from the distance duality bounds of refs. [14, 22]. With $\beta = -2\epsilon/3$, combining the most recent SN and $H(z)$ data (namely, the SCP Union2 Compilation [44] together with the latest $H(z)$ [39] data and Hubble parameter determination [45]) yields

$$\beta = 0.01 \pm 0.04\,, \tag{5.4}$$

at 95% confidence.

JCAP02(2012)013

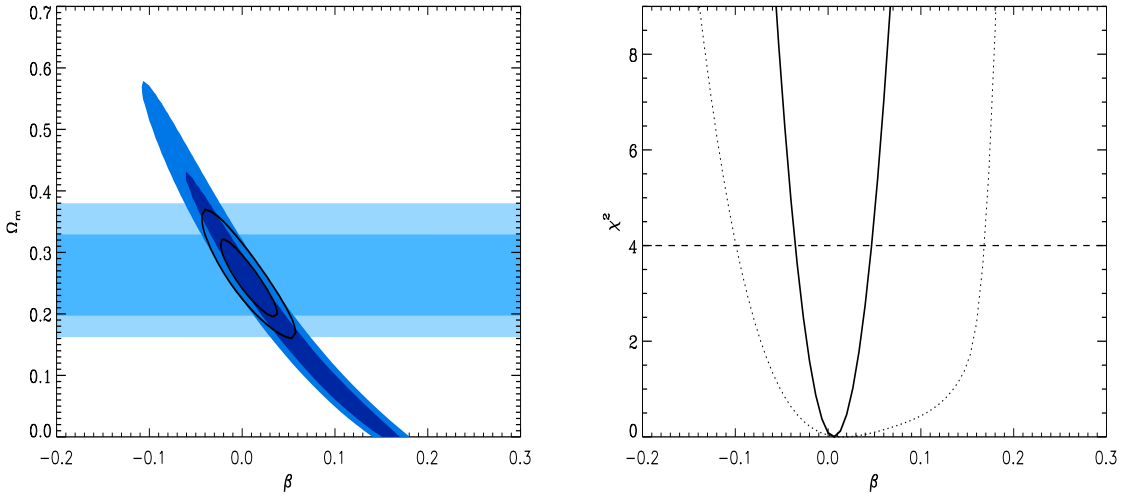

Figure 1. Constraints from SN+$H(z)$ on the parameter β, parameterising violations of the temperature-redshift relation as $T(z) = T_0(1+z)^{1-\beta}$. *Left*: two-parameter constraints on the β–Ω_m plane. Dark blue contours correspond to 68% and 95% confidence levels obtained from SN data alone, light blue contours are for $H(z)$ data, and solid line transparent contours show the joint SN+$H(z)$ constraint. *Right*: one-parameter joint constraints on β marginalised over cosmological parameters. The solid line is for SN+$H(z)$ while the dotted one for SN data only. The dashed line shows the $\Delta\chi^2 = 4$ level.

This has been obtained by considering flat ΛCDM models and marginalising over the matter density Ω_m and Hubble parameter H_0. Figure 1 shows the relevant constraint on the β–Ω_m plane after marginalising over H_0 (left) and the constraint (5.4) on β, obtained by marginalising over both H_0 and Ω_m. On the left, the dark blue contours are the 1 and 2-σ joint (2-parameter) confidence levels for the SN data, the lighter blue regions show the corresponding constraints from $H(z)$ data, and the solid black lines show the combined SN+$H(z)$ constraints. Again, as we will discuss in section 6.2, there are very good prospects for future improvements.

6 Forecasts

Having discussed the current constraints on the parameter β, we now move on to study in detail the prospects for improvements coming from the next generation of space and ground-based experiments. We will discuss in succession three different probes, which together span the redshift range $z \sim 0$–4. By combining data from different observations one can therefore explore thoroughly a wide range of redshifts and significantly reduce the statistical uncertainties on the underlying phenomenological parameters. Moreover, given the very different nature of each type of measurements, one also has a much better control over possible systematics — this is particularly important in the event of a detection of deviations from the canonical behaviour.

6.1 Low redshifts: Planck HFI (clusters)

Planck HFI [46] was specifically designed from the beginning to measure the SZ effect in galaxy clusters [51]: the spectral coverage allows one to explore the positive and negative

JCAP02(2012)013

part of the spectral distortion, and it is optimally suited for cluster detection and to break cluster parameters degeneracy.

The full sky survey will provide us with a SZ catalog of thousands of clusters. The Planck early results [47] already provide us with a sample of 189 cluster candidates. Here we focus on a survey dedicated to a sample of well known clusters, for which X-ray and optical information is available, so dealing with a subsample of the Early Planck cluster catalog (ESZ).

A catalog of 166 clusters has been built by using BAX (X-ray Clusters Database) [48]:

Cluster name	
RA (J2000)	Right ascension
DEC (J2000)	Declination
z	redshift
$\mathbf{F_X}$	unabsorbed X-ray flux in ROSAT band (0.1–2.4) keV in units of (10^{-12} erg/s/cm^2)
Reference-$\mathbf{F_x}$	
$\mathbf{L_X}$	X-ray luminosity in the ROSAT band (0.1–2.4) keV in 10^{44} ergs s^{-1}
Reference-$\mathbf{L_x}$	
Band-Inf (keV)	
Band-Sup (keV)	
$\mathbf{T_X}$	X-ray gas temperature in keV
$\boldsymbol{\sigma_{T_X}}$	
Reference-$\mathbf{T_x}$	
Instrument	
$\mathbf{R_{core}}$	Core Radius (arcsec)
$\boldsymbol{\sigma_{R_{core}}}$	
Reference-$\boldsymbol{R_{core}}$	
$\boldsymbol{\beta}$	slope of the gas density profile derived from the β-model fitting
$\boldsymbol{\sigma_\beta}$	

To avoid confusion, note that this β-model does not refer to the same β parameter as is discussed in the rest of the paper.

For each cluster we derive the following parameters:

$\boldsymbol{n_{e0}}$	central electronic density, assuming a isothermal β-model and following [49]
$\boldsymbol{y_{th}}$	central Comptonisation parameter
$\boldsymbol{\tau_{th}}$	central optical depth
$\boldsymbol{Y_{int}}$	Comptonisation parameter integrated over the cluster extent
$\mathbf{D_{A_{SZX}}}$	Angular distance

We have simulated the observations of a sample of about 40 well known clusters, already observed by Planck [47], taking into account the Planck HFI instrumental characteristics and observing strategy [50]. The frequency bands considered in the simulation are

JCAP02(2012)013

the four at lower frequencies (100, 143, 217, 353 GHz), since the remaining two higher frequency bands (545, 857 GHz) are best suited for foregrounds extraction and are not useful for the reconstruction of the SZ signal. CMB and foregrounds are assumed as previously removed.

The forecast for the SZ effect signal for the clusters has been obtained from the measured X-ray properties, assuming an isothermal model. The ICM pressure profile has historically been described by an isothermal β-model [52]. Recent X-ray observations have shown that a β-profile for gas density is a poor approximation for the cluster's profile at large radii, leading several authors to propose more realistic profiles [53, 54]. The use of the β-model in this work is for consistency with the X-ray derived parameters collected in the catalogue, which almost invariably were based on a β profile assumption for gas. Nevertheless, the analysis procedure to determine T(z) makes use of the central τ values, and it will not be affected by a different adopted profile.

We have used the Planck noise model (NET values as reported in [50]) to estimate the errors in the observed spectra. The integration time for the mock observation is obtained assuming uniform sky coverage and two years of observation. For each cluster the observation time is 10 s. The dilution effect has been taken into account to estimate the error on the SZ signal for each channel.

The mock dataset was then analysed to recover the original input parameters of the cluster. The analysis has been performed through a Monte Carlo Markov Chain (MCMC) algorithm which allows us to explore the full space of the cluster parameters (optical depth τ, peculiar velocity $v_{\rm pec}$, electron temperature T_e) and the CMB brightness temperature at the redshift of the cluster. In the analysis we allowed for calibration uncertainty, considered as an uncertain scale factor, which was modelled as a Gaussian with mean 1 and 0.1% standard deviation.[2]

The MCMC generates random sequences of parameters, which simulate posterior distributions for all parameters [57]. The sampling approach we used is the one proposed by Metropolis and Hastings [58, 59]. Convergence and mixing of the MCMC runs was tested through the Gelman-Rubin test [60]. We included a prior over the cluster gas temperature, as provided by X-ray data. For the radial component of the cluster peculiar velocities the prior is a theoretical one, a Gaussian with a universal vanishing mean and with a 1000 km/s standard deviation. Clusters with almost flat τ posterior are excluded from the sample (this is the reason for which the sample is different when the kinematic component is included from that when it is not included).

As was already noted in [5] there is a degeneracy between $T_{\rm CMB}(z)$ and $v_{\rm pec}$, see figure 2. In order to reduce the impact of this degeneracy and then to reduce the uncertainty in the determination of $T_{\rm CMB}(z)$, a better knowledge of the peculiar velocity is required or it is necessary to remove the kinematic component from the thermal component, together with the CMB intrinsic anisotropy. With only Planck measurements, given the multifrequency coverage, we can envisage the second option. Kinematic SZ (KSZ) and the intrinsic CMB anisotropy have the same spectral shape in the non relativistic limit; to separate the two components in nearby clusters or in distant clusters using beams larger than few arcmin it is necessary to rely on the very small spectral distortions of the kinematic SZ

[2]The adopted value for the absolute calibration accuracy is in a way too optimistic with respect to HFI early maps ($\leq 2\%$) [55], but still very conservative with respect to expected performances [56]. However, the impact of absolute calibration accuracy will mainly influence the τ parameter estimation, since ΔI depends linearly on τ at the first order.

JCAP02(2012)013

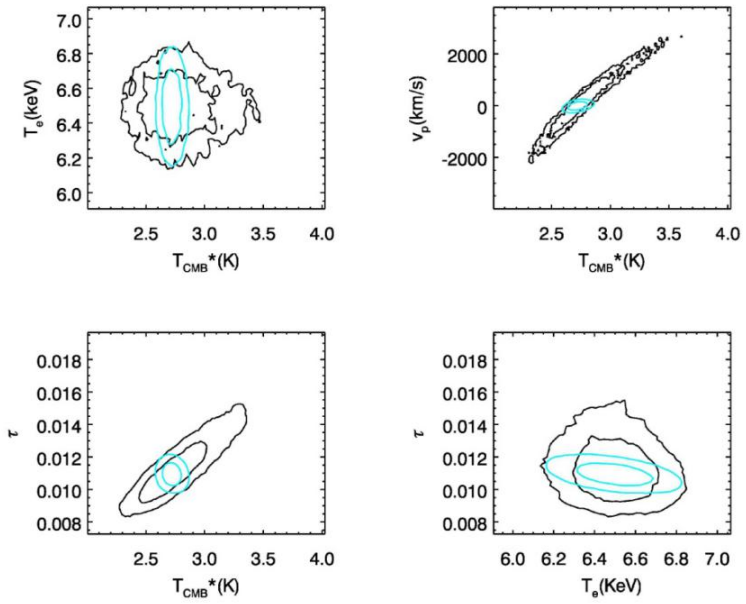

Figure 2. Parameter correlations for a simulated cluster: the contours show the 68% and 95% confidence limits from the marginalised distributions. Black (dark) contours are obtained allowing for a peculiar velocity prior with vanishing mean and standard deviation 1000 km/s; cyan (light) contours are obtained allowing for a peculiar velocity prior with vanishing mean and standard deviation 100 km/s. $T^*_{\rm CMB}$ corresponds to $T(z)/(1+z)$.

due to relativistic effects [61]. For Planck it is safe to consider that in a large majority of cases the spectral distortions of KSZ due to relativistic effects are too small with respect to CMB confusion and noise level to allow disentangling KSZ and CMB intrinsic anisotropy, i.e. the kinematic component is removed as a first step in cleaning maps of CMB contribution.

Nevertheless, in the following we will consider both cases, thus fitting either four parameters (τ, T_e, $v_{\rm pec}$, $T_{\rm CMB}(z)$) or three parameters (τ, T_e, $T_{\rm CMB}(z)$).

In figures 3 and 4 we present the results of the parameter estimation analysis for a single cluster, both with and without the kinematic component. In figures 5 and 6 we show the residuals for cluster parameters for the whole sample.

To obtain β we have performed a fit of the $T(z)$ data points (see figures 7 and 8). The final β value we get by fitting the $T(z)$ data points obtained with the MCMC treatment is $\beta = -0.047 \pm 0.079$ when the kinematic component is included (from a final sample of 19 clusters, selected with the condition of non flat τ posterior and $S/N \geq 6$) and $\beta = -0.003 \pm 0.016$ when the kinematic component is previously removed (from a final sample of 37 clusters, selected with the condition of non flat τ posterior and $S/N \geq 6$).

In conclusion, if the kinematic component is removed altogether with the CMB primary anisotropy component, with Planck we can reach 0.6% sensitivity on $T_{\rm CMB}(z)$ measurements; otherwise the sensitivity will be around 7%. With only tens of clusters we can in principle get better constraints on β than the current results with SZ+Atomic carbon+CO.

JCAP02(2012)013

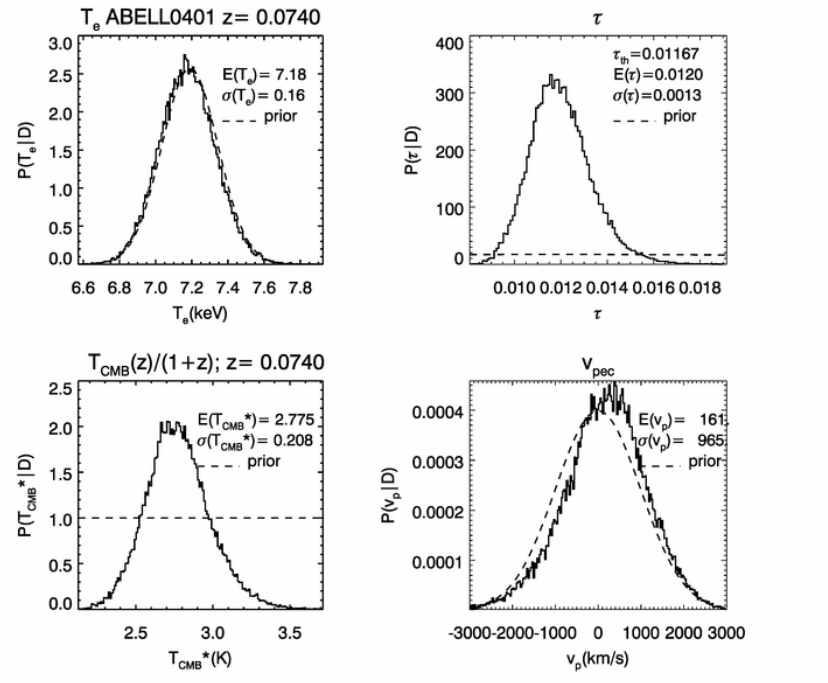

Figure 3. An example of parameter extraction for a single cluster, with kinematic component included.

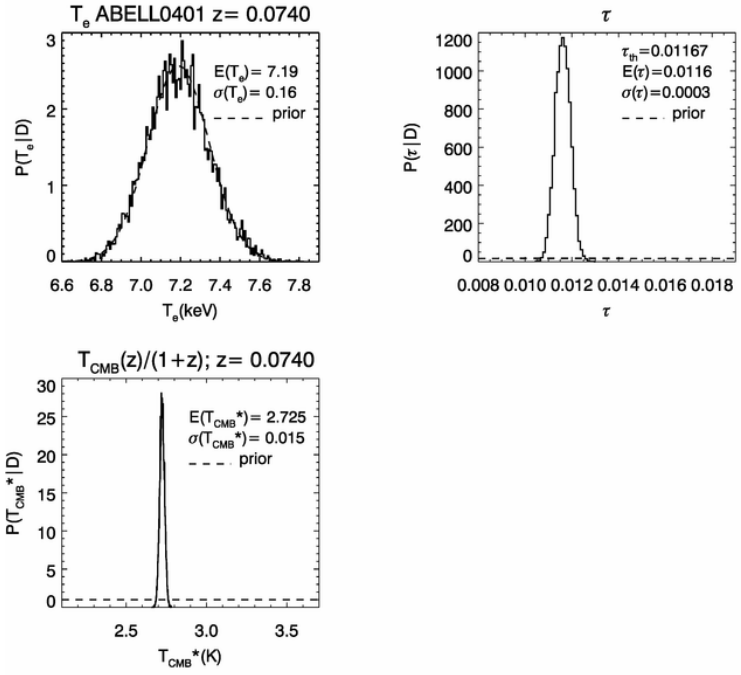

Figure 4. An example of parameter extraction for the same cluster of figure 3, with kinematic component not included.

JCAP02(2012)013

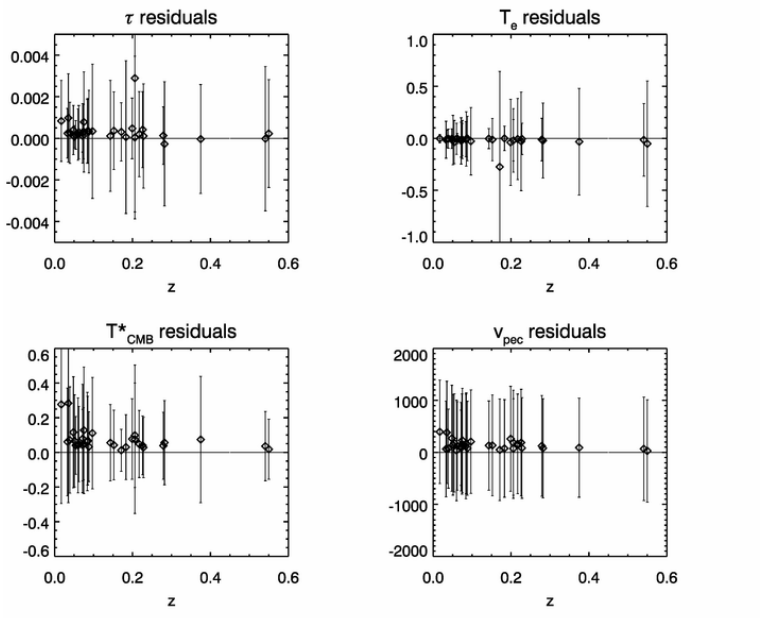

Figure 5. Residuals for 32 clusters, with kinematic component included. All the clusters with almost flat τ posterior have been excluded from the original 42-cluster sample.

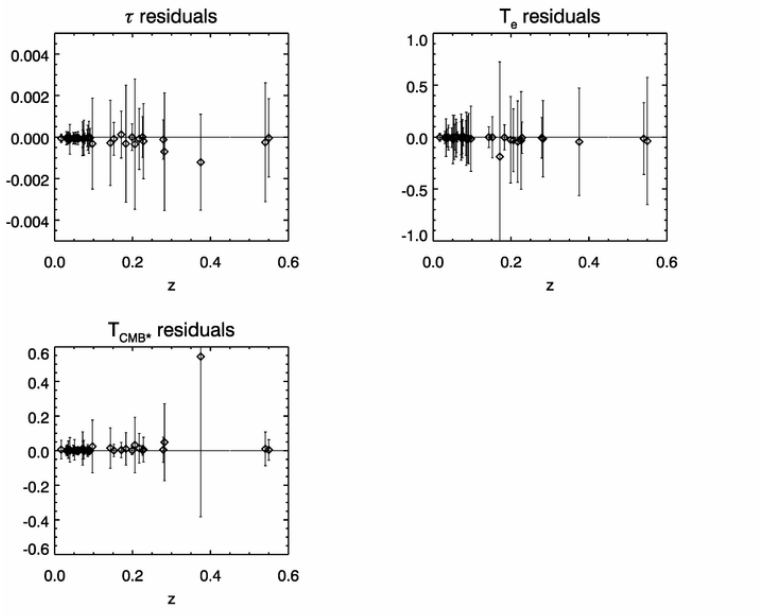

Figure 6. Residuals for 37 clusters, with kinematic component previously removed. All the clusters with almost flat τ posterior are excluded from the original 42-cluster sample.

JCAP02(2012)013

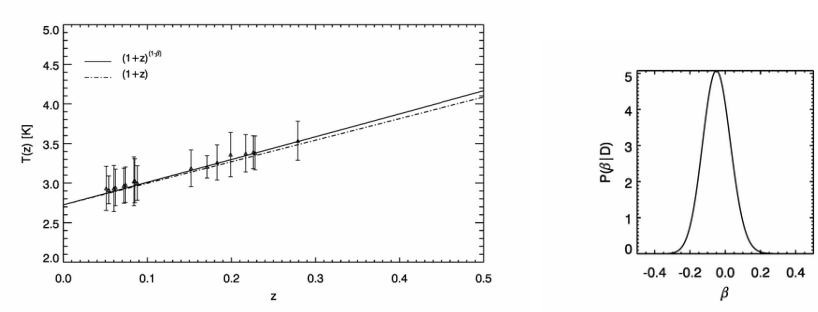

Figure 7. *Left*: $T_{\rm CMB}$ vs z, with the kinematic component included. *Right*: posterior of the β parameter, as obtained by performing a fit of the $T(z)$ data points.

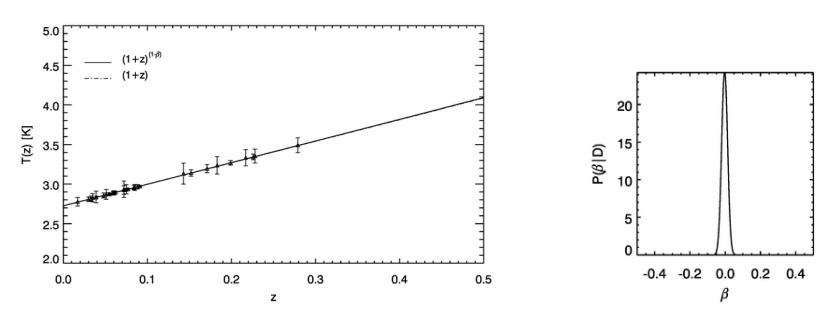

Figure 8. *Left*: $T_{\rm CMB}$ vs z, with the kinematic component not included. *Right*: posterior of the β parameter, as obtained by performing a fit of the $T(z)$ data points.

6.2 Intermediate redshifts: EUCLID/SNAP (distance measurements)

In this section, we show forecast constraints on the temperature-redshift relation (in particular on the parameter β of section 2) which could be achieved by combining $H(z)$ measurements from upcoming spectroscopic BAO surveys with future SN data. The next decade will see a dramatic improvement on $H(z)$ and angular diameter distance data at redshifts $z \lesssim 2$, notably through ongoing and upcoming BAO surveys like BOSS [62] and EUCLID [63]. Similarly, future SN missions (e.g. SNAP [64]) will dramatically reduce the errors in SN brightness data.

As discussed in [22], BOSS will not significantly improve opacity bounds (on which our constraint on β are based) with respect to current $H(z)$ cosmic chronometer data (i.e. from differential ageing of luminous red galaxies [39]), because it will be restricted to redshifts $z \leq 0.7$.

On the other hand EUCLID — a combination of the earlier SPACE [65] and DUNE [66] missions — will reach much higher redshifts and is expected to dramatically improve these constraints. Aiming for launch in 2019, it would cover about 20,000 deg^2 of sky providing around 150 million redshifts in the range $z < 2$. Here, we consider forecast constraints from EUCLID and a Supernova SNAP-like survey (or dark energy task force stage IV SNe mission) [67].

We use the code developed by Seo & Eisenstein [68] to estimate the errors in radial distances achievable by using BAO as a standard ruler. Figure 9 shows our forecasted constraints on the parameter β, using modelled BAO data with forecasted errors for EUCLID, combined with modelled SN data and errors for a SNAP-like survey.

JCAP02(2012)013

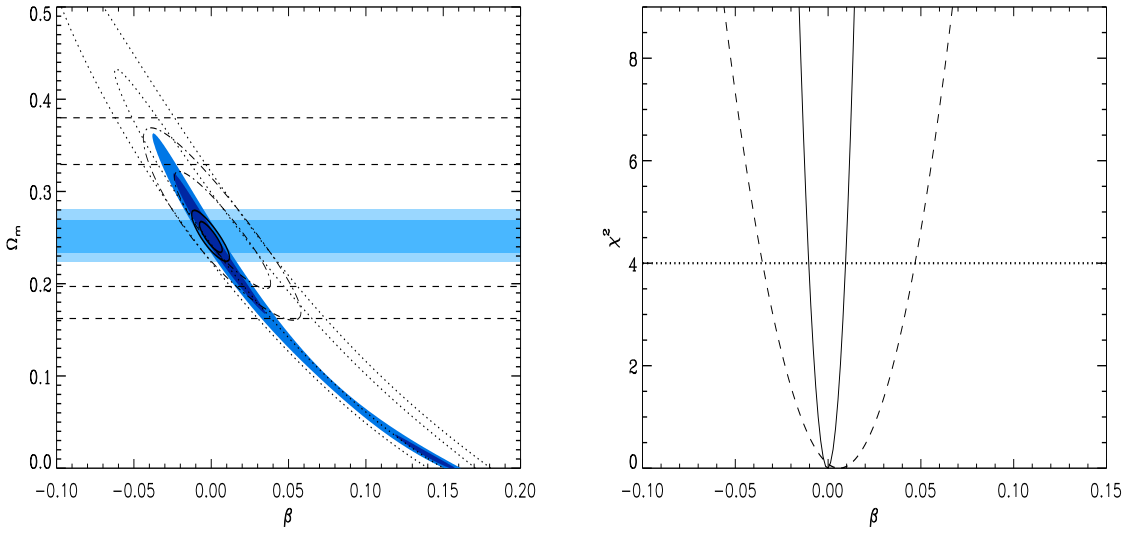

Figure 9. Future constraints on the parameter β from EUCLID and SNAP. *Left*: two-parameter constraints on the β–Ω_m plane. Dark blue contours correspond to 68% and 95% confidence levels from SNAP alone, light blue contours are for EUCLID, and solid line transparent contours show the joint SNAP+EUCLID forecast constraint. Also shown are current constraints from $H(z)$ 'chronometer' data (dashed), SN data (dotted), and joint $H(z)$+SN (dot-dashed), presented in section 5, figure 1. *Right*: one-parameter joint constraints on β marginalised over cosmological parameters. The solid line shows the forecast constraint from EUCLID+SNAP, while the dashed line corresponds to the current constraint from $H(z)$+SN, discussed in section 5, figure 1. The dashed line is the 95% confidence level.

On the left panel, light blue contours show the 1-σ and 2-σ (2-parameter) constraints on the β–Ω_m plane from EUCLID only, darker blue contours show the corresponding constraints from SNAP, while solid line transparent contours show the (2-parameter) joint EUCLID+SNAP forecast constraints. To make a more direct comparison we have also shown the corresponding constraints obtained from current data, namely 'cosmic chronometer' $H(z)$ (dashed), SN (dotted), and joint $H(z)$+SN (dot-dashed), discussed in section 5. The right panel shows the relevant 1-parameter constraint on β, after marginalising over Ω_m, for EUCLID+SNAP (solid) and current $H(z)$+SN data (dashed). The dotted line is the 95% confidence level, $\Delta\chi^2 = 4$.

Overall, the improvement with respect to current constraints by combining EUCLID+SNAP will be quite significant, with the area of the joint constraint in figure 9 (left) reduced by a factor of a few decades. The one parameter constraint on β will be improved by a factor $\gtrsim 5$, reaching $|\Delta\beta| \sim 0.008$ at 95% confidence. This is competitive to the Planck HFI result, discussed above.

6.3 High redshifts: ESPRESSO and CODEX (spectroscopy)

ESPRESSO[3] (for the VLT) and CODEX[4] (for the E-ELT) are two forthcoming ESO high-resolution, ultra-stable spectrographs. Although their common cosmology-related science

[3]See http://espresso.astro.up.pt/.
[4]See http://www.iac.es/proyecto/codex/.

JCAP02(2012)013

driver is the precise spectroscopic measurement of nature's fundamental couplings (particularly the fine-structure constant α and the proton-to-electron mass ratio μ, see [69]), they will be in a unique position to carry out precise measurements of $T(z)$ at high redshift.

As discussed in section 3, there are currently 5 CO absorption systems, in the redshift range $z \sim 1.5$–3.0, where the CMB temperature can be measured with an uncertainty

$$\Delta T_{\rm Now} \sim 0.7\,{\rm K}\,. \tag{6.1}$$

Based on current plans for ESPRESSO and CODEX [70–72], we can estimate that they will be able to reduce this uncertainty to, respectively,

$$\Delta T_{\rm ESP} \sim 0.35\,{\rm K} \tag{6.2}$$

and

$$\Delta T_{\rm COD} \sim 0.07\,{\rm K}\,. \tag{6.3}$$

Given the planned redshift range of both spectrographs, their measurements will on average be done at higher redshifts, and here we will assume a redshift range $z \sim 2.8$–4.0; from a theoretical point of view, going to higher redshifts is obviously desirable since they provide a bigger lever arm; however, one also has to keep in mind that these systems will be fainter.

Having said that, it is important to realise that the bottleneck here is not the amount of telescope time required to observe these systems (although that naturally grows as systems become fainter). In fact, in some systems that are observed with the aim of measuring μ one can also measure $T(z)$, so there could in fact be no extra cost in terms of telescope time. Instead, the bottleneck is simply finding more systems where these measurements can be made. Ongoing surveys such as SDSS-III BOSS [62] can play an important role in this endeavour. For the purposes of the present analysis we will assume that ESPRESSO will accurately measure $T(z)$ in 10 systems, while CODEX will measure 20 systems.

One can then generate mock catalogs of $T(z)$ measurements, assuming the standard scenario as a fiducial model and the above temperature uncertainties and redshift ranges, and determine the constraint on β that such a catalog can yield. For simplicity we also assume a uniform probability in the redshift distribution of the sources. We will also assume that the uncertainty in the measurement at $z = 0$ remains unchanged. Naturally, the constraint will have a mild dependence on where in the allowed redshift range the small number of sources happen to fall, but by generating a large number of realisations one can infer a representative uncertainty on β.

The results of this analysis are summarised in figure 10: ESPRESSO is expected to improve on the constraints coming from currently available spectroscopic measurements by a factor of 3, and CODEX should improve on ESPRESSO by another factor of 3. As stated above, if more systems are found where the spectrographs can make these measurements, one could in principle further improve the sensitivity on β.

7 Summary: current and future constraints

We are now in a position to summarise the constraints on allowed deviations from the standard temperature-redshift relation. By combining the direct constraints from Noterdaeme et al. [8] with the indirect ones that we have obtained in section 5, we finally obtain the weighted mean result

$$\beta = 0.004 \pm 0.016\,, \tag{7.1}$$

JCAP02(2012)013

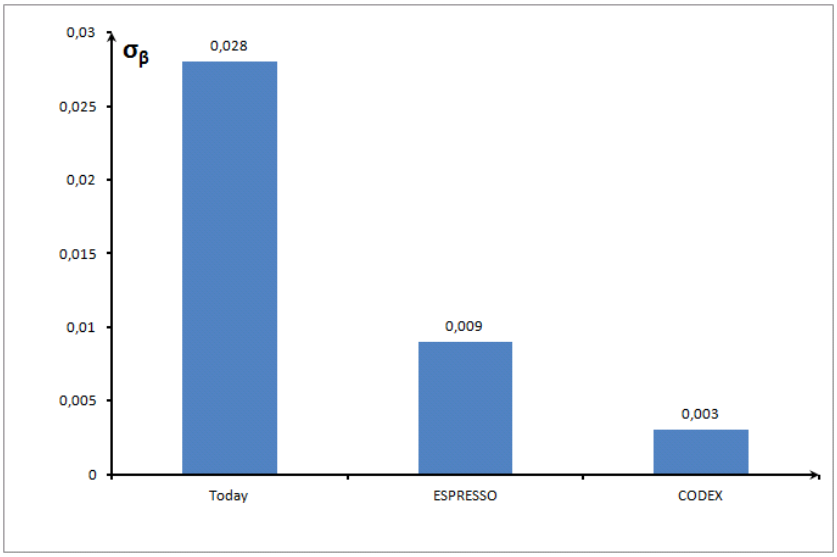

Figure 10. Forecasts for direct constraints on the phenomenological parameter β for ESPRESSO and CODEX, compared with the current uncertainty (coming from combining all available direct measurements, cf. section 4).

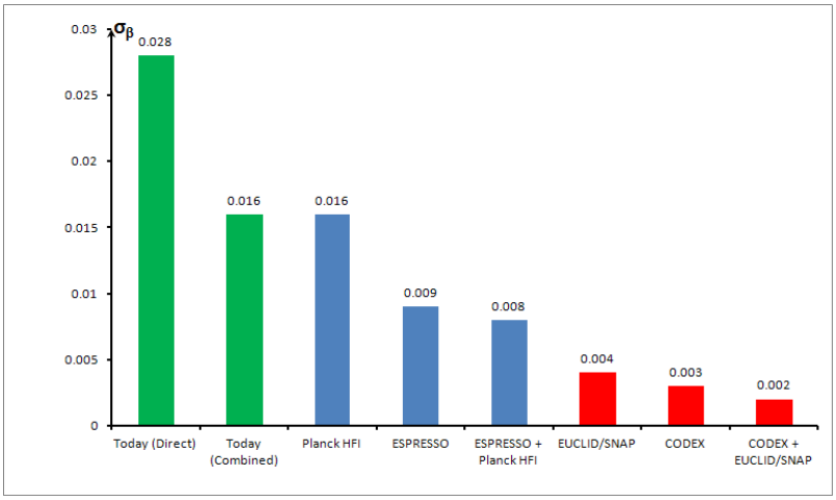

Figure 11. Comparing the current one-sigma uncertainties on the parameter β (from direct measurements and from a combination of direct and indirect ones) with that achievable by ongoing and future experiments, specifically Planck HFI and ESPRESSO in the near future and EUCLID/SNAP and CODEX in the longer term.

which is a 40% improvement on the direct constraint. We note that the three observational methods (clusters, distance measurements and spectroscopy) are nicely complementary, not only in terms of possible systematic uncertainties but also in terms of the redshift ranges covered. These results are summarised in figure 11, and compared with the forecasts for the various future experiments that we discussed in the previous section.

For experiments whose results will be available before 2020, we have considered Planck HFI and the ESPRESSO spectrograph. One can see that Planck alone should be able to do as

JCAP02(2012)013

well as all the current data, with only tens of clusters. When ESPRESSO becomes available, it will allow a gain of a factor of 3 in sensitivity relative to the current direct constraints, and a factor of 2 relative to the constraints available just before it.

We point out that the Early SZ Planck catalogue [73] consists of 189 clusters and it is obtained with a selection criterion of S/N > 6, thus implying that the SZ cluster sample for which $T_{\rm CMB}$ can be extracted is at least a factor of 4 larger than the one presented in this work; assuming that the spanned redshift range is the same as the one taken into account here (thus sensitivity on $T_{\rm CMB}(z)$ measurements is almost unchanged) then we have a 50% improvement on the constrained β ($\sigma_\beta \sim 0.008$). Spatially resolved spectroscopic observations of galaxy clusters (as proposed with SAGACE [74] or Millimetron[5]) would allow to further improve these constraints. Finally, we note that there are also other techniques that can in principle be used to obtain these constraints from SZ clusters [75].

In the longer (post-2020) term, CODEX and a combination of EUCLID and a SNAP-like survey will bring significant further improvements. Here the order in which they will become available is uncertain (as are, to some extent, their detailed characteristics), but their combined results are expected to bring a gain of about an order of magnitude relative to current sensitivities and of factors between 2 and 4 relative to the constraints available just before them.

Our analysis may in some ways be too simplistic, but we emphasise that in other ways it is fairly conservative. This is particularly the case when it comes to the assumptions on the number of systems in which the measurements can be made. The Early SZ Planck catalogue is evidence of this fact for the low redshift range, but the same is true for the spectroscopic measurements at high redshift. Given the exquisite resolution and stability of the forthcoming ESO spectrographs and the large redshift lever arm they can probe, the most cost-effective way to further improve these constraints is undoubtedly to identify further systems where ESPRESSO and CODEX can make these measurements.

8 Conclusions

In this paper we have explored novel techniques for constraining physics beyond the standard model, focusing, in particular, on cosmological scenarios that can violate photon number conservation. These include — but are not limited to — models in which photons mix with axion-like particles, decaying vacuum cosmologies and other photon injection mechanisms, models with astrophysical dust, and so on. By noting that such models can simultaneously modify the cosmological distance duality relation and the CMB temperature scaling law (these modifications being parametrically related to each other), we have initiated a programme of studying the consistency of these models through a combination of direct and indirect probes. Relevant probes include SN brightness measurements (yielding luminosity distances), galaxy ageing and/or BAO techniques (giving radial and angular diameter distances), SZ measurements of galaxy clusters (providing $T(z)$ at low redshifts $0<z<1$) and quasar absorption line spectroscopy (measuring $T(z)$ at higher redshifts up to $z \sim$ a few).

This significantly enlarges ones' toolbox for studying cosmological models beyond the standard paradigm and leads to a notable improvement on current constraints on such models. Indeed, the probes used are complementary, each having different systematics and/or

[5]See http:/www.sron.rug.nl/millimetron.

JCAP02(2012)013

redshift cover, so combining data from several probes allows one to reduce systematic uncertainties and obtain more stringent consistency checks, as well as improved constraints on the models under study. The combined bound (7.1), which we have obtained on the parameter β quantifying deviations from the standard $T(z)$ law (see equation (2.15)), is a 40% improvement over the corresponding direct constraints in [8].

The potential of this programme is enormous. Considering ongoing and future missions (Planck HFI, EUCLID, SNAP, ESPRESSO, CODEX) we have obtained forecast constraints/errors on the parameter β. The expected improvement in current 1-σ error bars can be up to two orders of magnitude, as summarised in figure 11. There is also room for expanding further the current toolbox by accommodating more probes, again with different systematics and redshift cover. For example, the position of the first acoustic peak in the CMB is also sensitive to distance duality violations and so provides a new tool at the redshift of last scattering [76].

In this work, we have only tried to demonstrate the effectiveness of these techniques by considering simple parameterisations, which are not necessarily physically motivated. These may be adequate for work with currently available data, but as redshift cover increases and sensitivity improves, better parameterisations will be required. However, it is important to highlight that, even with current sensitivity, the techniques described here have a notable potential for constraining specific cosmological and high-energy physics models beyond the standard paradigm if specific 'model-tailored' parameterisations are used. Within a given model, the underlying physics often points to specific parameterisations for the violation of standard laws, and these parameters can be directly related to fundamental/microphysical parameters of the underlying theory. This approach was initiated in reference [22], where specific parameterisations for distance duality violation were adopted for different models (photon-axion mixing, hidden photons, mini-charged particles). Other scenarios that can be probed with the tools described in this paper, through the use of more realistic parameterisations as suggested by the theory, include varying α cosmologies and dynamical dark energy. These will be discussed in detail in a follow-up publication [77].

Acknowledgments

This work was done in the context of the cooperation grants 'Evolution and Astrophysical Consequences of Cosmic Strings and Superstrings' (CRUP/British Council ref. B-13/10), and 'Probing Fundamental Physics with Planck' (PHC-EGIDE/Programa PESSOA, grant FCT/1562/25/1/2012/S).

A.A. was supported by a CTC Postdoctoral Fellowship at DAMTP, University of Cambridge and in part by a Marie Curie IEF Fellowship at the the University of Nottingham. The work of G.L. is funded by a CNRS Postdoctoral Fellowship at LAL, Centre Scientifique d'Orsay. The work of C.M. is funded by a Ciência2007 Research Contract, supported by FCT/MCTES (Portugal) and POPH/FSE (EC). The work of A.M.M. was partially funded by Grant No. CAUP-03/2011-BII.

This research has made use of the X-Rays Clusters Database (BAX) which is operated by the Laboratoire d'Astrophysique de Tarbes-Toulouse (LATT), under contract with the Centre National d'Etudes Spatiales (CNES). We also acknowledge useful discussions on $T(z)$ measurements with Paolo Molaro and Patrick Petitjean, particularly for defining the observational scenarios for ESPRESSO and CODEX.

JCAP02(2012)013

References

[1] J.C. Mather et al., *Measurement of the cosmic microwave background spectrum by the COBE FIRAS instrument*, *Astrophys. J.* **420** (1994) 439 [INSPIRE].

[2] J. Jaeckel and A. Ringwald, *The low-energy frontier of particle physics*, *Ann. Rev. Nucl. Part. Sci.* **60** (2010) 405 [arXiv:1002.0329] [INSPIRE].

[3] C.J.A.P. Martins, *Cosmology with varying constants*, *Phil. Trans. Roy. Soc. Lond.* **A 360** (2002) 2681 [astro-ph/0205504] [INSPIRE].

[4] E.S. Battistelli et al., *Cosmic microwave background temperature at galaxy clusters*, *Astrophys. J.* **580** (2002) L101 [astro-ph/0208027] [INSPIRE].

[5] G. Luzzi et al., *Redshift dependence of the CMB temperature from S-Z measurements*, *Astrophys. J.* **705** (2009) 1122 [arXiv:0909.2815] [INSPIRE].

[6] C. Horellou, M. Nord, D. Johansson and A. Lévy, *Probing the cosmic microwave background temperature using the Sunyaev-Zeldovich effect*, *Astron. Astrophys.* **441** (2005) 435 [astro-ph/0507032] [INSPIRE].

[7] R. Srianand, P. Petitjean and C. Ledoux, *The microwave background temperature at the redshift of 2.33771*, *Nature* **408** (2000) 931 [astro-ph/0012222] [INSPIRE].

[8] P. Noterdaeme, P. Petitjean, R. Srianand, C. Ledoux and S. López, *The evolution of the cosmic microwave background temperature. Measurements of $T_{\rm CMB}$ at high redshift from carbon monoxide excitation*, *Astron. Astrophys.* **526** (2011) L7 [arXiv:1012.3164] [INSPIRE].

[9] I.M.H. Etherington, *On the definition of distance in general relativity*, *Phil. Mag.* **15** (1933) 761.

[10] J.A.S. Lima, *Thermodynamics of decaying vacuum cosmologies*, *Phys. Rev.* **D 54** (1996) 2571 [gr-qc/9605055] [INSPIRE].

[11] J.A.S. Lima, A.I. Silva and S.M. Viegas, *Is the radiation temperature redshift relation of the standard cosmology in accordance with the data?*, *Mon. Not. Roy. Astron. Soc.* **312** (2000) 747 [INSPIRE].

[12] A.N. Aguirre, *Dust vs. cosmic acceleration*, *Astrophys. J.* **512** (1999) L19 [astro-ph/9811316] [INSPIRE].

[13] Supernova Cosmology Project collaboration, M. Kowalski et al., *Improved cosmological constraints from new, old and combined supernova datasets*, *Astrophys. J.* **686** (2008) 749 [arXiv:0804.4142] [INSPIRE].

[14] A. Avgoustidis, L. Verde and R. Jimenez, *Consistency among distance measurements: transparency, BAO scale and accelerated expansion*, *JCAP* **06** (2009) 012 [arXiv:0902.2006] [INSPIRE].

[15] P. Svrček and E. Witten, *Axions in string theory*, *JHEP* **06** (2006) 051 [hep-th/0605206] [INSPIRE].

[16] C. Csáki, N. Kaloper and J. Terning, *Dimming supernovae without cosmic acceleration*, *Phys. Rev. Lett.* **88** (2002) 161302 [hep-ph/0111311] [INSPIRE].

[17] L. Ostman and E. Mortsell, *Limiting the dimming of distant type Ia supernovae*, *JCAP* **02** (2005) 005 [astro-ph/0410501] [INSPIRE].

[18] A. Mirizzi, G.G. Raffelt and P.D. Serpico, *Photon-axion conversion as a mechanism for supernova dimming: limits from CMB spectral distortion*, *Phys. Rev.* **D 72** (2005) 023501 [astro-ph/0506078] [INSPIRE].

[19] A. Mirizzi, J. Redondo and G. Sigl, *Constraining resonant photon-axion conversions in the early universe*, *JCAP* **08** (2009) 001 [arXiv:0905.4865] [INSPIRE].

JCAP02(2012)013

[20] A. Mirizzi, J. Redondo and G. Sigl, *Microwave background constraints on mixing of photons with hidden photons*, *JCAP* **03** (2009) 026 [arXiv:0901.0014] [INSPIRE].

[21] H. Georgi, P.H. Ginsparg and S.L. Glashow, *Photon oscillations and the cosmic background radiation*, *Nature* **306** (1983) 765 [INSPIRE].

[22] A. Avgoustidis, C. Burrage, J. Redondo, L. Verde and R. Jimenez, *Constraints on cosmic opacity and beyond the standard model physics from cosmological distance measurements*, *JCAP* **10** (2010) 024 [arXiv:1004.2053] [INSPIRE].

[23] B.A. Bassett and M. Kunz, *Cosmic acceleration vs. axion-photon mixing*, *Astrophys. J.* **607** (2004) 661 [astro-ph/0311495] [INSPIRE].

[24] B.A. Bassett and M. Kunz, *Cosmic distance-duality as a probe of exotic physics and acceleration*, *Phys. Rev.* **D 69** (2004) 101305 [astro-ph/0312443] [INSPIRE].

[25] S. More, J. Bovy and D.W. Hogg, *Cosmic transparency: a test with the baryon acoustic feature and type-IA supernovae*, *Astrophys. J.* **696** (2009) 1727 [arXiv:0810.5553] [INSPIRE].

[26] D.J. Fixsen et al., *The cosmic microwave background spectrum from the full COBE FIRAS data set*, *Astrophys. J.* **473** (1996) 576 [astro-ph/9605054] [INSPIRE].

[27] K.C. Roth and D.M. Meyer, *Cyanogen excitation in diffuse interstellar clouds*, *Astrophys. J.* **441** (1995) 129.

[28] D.E. Welty, S.R. Federman, R.Gredel, J.A. Thorburn and D.L. Lambert, *VLT UVES observations of interstellar molecules and diffuse bands in the Magellanic Clouds*, *Astrophys. J. Suppl.* **165** (2006) 138 [astro-ph/0603332] [INSPIRE].

[29] J.N. Bahcall and R.A. Wolf, *Fine-structure transitions*, *Astrophys. J.* **152** (1968) 701.

[30] P. Molaro, S.A. Levshakov, M. Dessauges-Zavadsky and S. D'Odorico, *The cosmic microwave background radiation temperature at $z_{\rm abs} = 3.025$ toward QSO 0347-3819*, *Astron. Astrophys.* **381** (2002) L64 [astro-ph/0111589] [INSPIRE].

[31] A. Omont, *Molecules in galaxies*, *Rept. Prog. Phys.* **70** (2007) 1099 [arXiv:0709.3814] [INSPIRE].

[32] R. Srianand, P. Noterdaeme, C. Ledoux and P. Petitjean, *First detection of CO in a high-redshift damped Lyman-α system*, *Astron. Astrophys.* **482** (2008) L39.

[33] R. Fabbri, F. Melchiorri and V. Natale, *The Sunyaev-Zel'dovich effect in the millimetric region*, *Astrophys. Space Sci.* **59** (1978) 223.

[34] Y. Rephaeli, *On the determination of the degree of cosmological Compton distortions and the temperature of the cosmic blackbody radiation*, *Astrophys. J.* **241** (1980) 858.

[35] V.A. Kostelecky and N. Russell, *Data tables for Lorentz and CPT violation*, *Rev. Mod. Phys.* **83** (2011) 11 [arXiv:0801.0287] [INSPIRE].

[36] C. Burrage, *Supernova brightening from chameleon-photon mixing*, *Phys. Rev.* **D 77** (2008) 043009 [arXiv:0711.2966] [INSPIRE].

[37] R. Jimenez, L. Verde, T. Treu and D. Stern, *Constraints on the equation of state of dark energy and the Hubble constant from stellar ages and the CMB*, *Astrophys. J.* **593** (2003) 622 [astro-ph/0302560] [INSPIRE].

[38] J. Simon, L. Verde and R. Jimenez, *Constraints on the redshift dependence of the dark energy potential*, *Phys. Rev.* **D 71** (2005) 123001 [astro-ph/0412269] [INSPIRE].

[39] D. Stern, R. Jimenez, L. Verde, M. Kamionkowski and S. Stanford, *Cosmic chronometers: constraining the equation of state of dark energy. I: H(z) measurements*, *JCAP* **02** (2010) 008 [arXiv:0907.3149] [INSPIRE].

[40] P.P. Kronberg, *Extragalactic magnetic fields*, *Rept. Prog. Phys.* **57** (1994) 325.

JCAP02(2012)013

[41] J.D. Barrow, P.G. Ferreira and J. Silk, *Constraints on a primordial magnetic field*, *Phys. Rev. Lett.* **78** (1997) 3610 [astro-ph/9701063] [INSPIRE].

[42] P. Blasi, S. Burles and A.V. Olinto, *Cosmological magnetic fields limits in an inhomogeneous universe*, *Astrophys. J.* **514** (1999) L79 [astro-ph/9812487] [INSPIRE].

[43] C. Csáki, N. Kaloper and J. Terning, *Effects of the intergalactic plasma on supernova dimming via photon axion oscillations*, *Phys. Lett.* **B 535** (2002) 33 [hep-ph/0112212] [INSPIRE].

[44] R. Amanullah et al., *Spectra and light curves of six type Ia supernovae at* $0.511 < z < 1.12$ *and the Union2 compilation*, *Astrophys. J.* **716** (2010) 712 [arXiv:1004.1711] [INSPIRE].

[45] A.G. Riess et al., *A 3% solution: determination of the Hubble constant with the Hubble Space Telescope and Wide Field Camera 3*, *Astrophys. J.* **730** (2011) 119 [*Erratum ibid.* **732** (2011) 129] [arXiv:1103.2976] [INSPIRE].

[46] J.-M. Lamarre et al., *Planck pre-launch status: the HFI instrument, from specification to actual performance*, *Astron. Astrophys.* **520** (2010) A9.

[47] PLANCK collaboration, P. Ade et al., *Planck early results. VII. The early release compact source catalog*, *Astron. Astrophys.* **536** (2011) A7 [arXiv:1101.2041] [INSPIRE].

[48] R. Sadat et al., *Introducing BAX: a database for X-ray clusters and groups of galaxies*, *Astron. Astrophys.* **424** (2004) 1097 [astro-ph/0405457] [INSPIRE].

[49] A. Furuzawa et al., *ASCA observation of the distant cluster of galaxies CL 0016+16 and implication for* H_0, *Astrophys. J.* **504** (1998) 35.

[50] European Space Agency, *Planck. The scientific programme*, ESA-SCI(2005)1.

[51] N. Aghanim, A. de Luca, F.R. Bouchet, R. Gispert and J.L. Puget, *Cosmology with Sunyaev-Zeldovich observations from space*, *Astron. Astrophys.* **325** (1997) 9 [astro-ph/9705092] [INSPIRE].

[52] A. Cavaliere and R. Fusco-Femiano, *The distribution of hot gas in clusters of galaxies*, *Astron. Astrophys.* **70** (1978) 677.

[53] D. Nagai, A.V. Kravtsov and A. Vikhlinin, *Effects of galaxy formation on thermodynamics of the intracluster medium*, *Astrophys. J.* **668** (2007) 1 [astro-ph/0703661] [INSPIRE].

[54] M. Arnaud et al., *The universal galaxy cluster pressure profile from a representative sample of nearby systems (REXCESS) and the* Y_{SZ}-M_{500} *relation*, *Astron. Astrophys.* **517** (2010) A92 [arXiv:0910.1234] [INSPIRE].

[55] PLANCK HFI CORE TEAM collaboration, *Planck early results. VI. The high frequency instrument data processing*, *Astron. Astrophys.* **536** (2011) A6 [arXiv:1101.2048] [INSPIRE].

[56] M. Tristram et al., *Iterative destriping and photometric calibration for Planck-HFI, polarized, multi-detector map-making*, *Astron. Astrophys.* **534** (2011) A88 [arXiv:1103.2281] [INSPIRE].

[57] A. Lewis and S. Bridle, *Cosmological parameters from CMB and other data: a Monte Carlo approach*, *Phys. Rev.* **D 66** (2002) 103511 [astro-ph/0205436] [INSPIRE].

[58] N. Metropolis, A.W. Rosenbluth, M.N. Rosenbluth, A.H. Teller and E. Teller, *Equation of state calculations by fast computing machines*, *J. Chem. Phys.* **21** (1953) 1087.

[59] W.K. Hastings, *Monte Carlo sampling methods using Markov chains and their applications*, *Biometrika* **57** (1970) 97.

[60] A. Gelman and D.B. Rubin, *Inference from iterative simulation using multiple sequences*, *Statist. Sci.* **7** (1992) 457.

[61] J.E. Carlstrom, G.P. Holder and E.D. Reese, *Cosmology with the Sunyaev-Zel'dovich effect*, *Ann. Rev. Astron. Astrophys.* **40** (2002) 643 [astro-ph/0208192] [INSPIRE].

JCAP02(2012)013

[62] SDSS-III collaboration, D. Schlegel, M. White and D. Eisenstein, *The Baryon Oscillation Spectroscopic Survey: precision measurements of the absolute cosmic distance scale*, arXiv:0902.4680 [INSPIRE].

[63] A. Refregier et al., *EUCLID Imaging Consortium science book*, arXiv:1001.0061 [INSPIRE].

[64] SNAP collaboration, G. Aldering et al., *Overview of the Supernova/Acceleration Probe (SNAP)*, astro-ph/0209550 [INSPIRE].

[65] A. Cimatti et al., *SPACE: the SPectroscopic All-sky Cosmic Explorer*, *Exper. Astron.* **23** (2009) 39 [arXiv:0804.4433] [INSPIRE].

[66] DUNE collaboration, A. Refregier and M. Douspis, *Summary of the DUNE mission concept*, arXiv:0807.4036 [INSPIRE].

[67] A. Albrecht et al., *Report of the dark energy task force*, astro-ph/0609591 [INSPIRE].

[68] H.-J. Seo and D.J. Eisenstein, *Improved forecasts for the baryon acoustic oscillations and cosmological distance scale*, *Astrophys. J.* **665** (2007) 14 [astro-ph/0701079] [INSPIRE].

[69] C.J.A.P. Martins and P. Molaro eds., *From varying couplings to fundamental physics: Proceedings of Symposium 1 of JENAM 2010*, Springer (2011).

[70] S. Cristiani et al., *The CODEX-ESPRESSO experiment: cosmic dynamics, fundamental physics, planets and much more*, *Nuovo Cim.* **B 122** (2007) 1159 [arXiv:0712.4152] [INSPIRE].

[71] J. Liske et al., *From ESPRESSO to CODEX*, arXiv:0802.1926 [INSPIRE].

[72] F.A. Pepe et al., *ESPRESSO: the Echelle spectrograph for rocky exoplanets and stable spectroscopic observations*, *Proc. SPIE* **7735** (2010) 77350F.

[73] PLANCK collaboration, P. Ade et al., *Planck early results. VIII. The all-sky early Sunyaev-Zeldovich cluster sample*, arXiv:1101.2024 [INSPIRE].

[74] P. De Bernardis et al., *SAGACE: the Spectroscopic Active Galaxies And Clusters Explorer*, in Proceedings of the *12th Marcel Grossmann Meeting*, Paris France, 12–18 July 2009 [arXiv:1002.0867] [INSPIRE].

[75] I. de Martino et al., *Measuring the redshift dependence of the CMB monopole temperature with Planck data*, in preparation.

[76] A. Avgoustidis, G. Luzzi and C.J.A.P. Martins, work in progress.

[77] A. Avgoustidis, G. Luzzi, C.J.A.P. Martins and A.M.R.V.L. Monteiro, *T(z) measurements can constrain varying-alpha and evolving dark energy models*, work in progress.

JCAP02(2012)013